Electrochemical Behavior of Solid Lithium Manganate (LiMn 2 O 4) in Aqueous Neutral Electrolyte Solutions

ARTICLE *in* LANGMUIR · SEPTEMBER 2003

Impact Factor: 4.46 · DOI: 10.1021/la0340448

3 AUTHORS, INCLUDING:

Mandapati Mohan Rao
Indian Institute of Chemical Technology
42 PUBLICATIONS **750** CITATIONS

Electrochemical Behavior of Solid Lithium Manganate ($LiMn_2O_4$) in Aqueous Neutral Electrolyte Solutions

M. Jayalakshmi,† M. Mohan Rao,*,† and F. Scholz‡

Indian Institute of Chemical Technology, Inorganic Division, Uppal Road, Hyderabad 500007, India, Institut für Chemie und Biochemie, Ernst-Moritz-Arndt-Universität Greifswald, Soldmannstrasse 23, D-17489 Greifswald, Germany

Received January 10, 2003. In Final Form: July 17, 2003

Lithium manganate ($LiMn_2O_4$) was synthesized by a very simple low-temperature solution combustion technique. The product was characterized for its phase formation and composition by X-ray diffraction and inductively coupled plasma spectroscopy. The electrochemical behavior of this material in aqueous neutral electrolyte solutions was investigated in an effort to find a means of making it a usable electrode material for rechargeable battery systems in aqueous electrolytes. Cyclic voltammetric and chronopotentiometric studies of solid $LiMn_2O_4$ immobilized on a paraffin-impregnated graphite electrode were carried out in various aqueous neutral electrolyte solutions. $LiMn_2O_4$ was shown to undergo reversible insertion of K^+, Li^+, and NH_4^+ ions from neutral electrolyte solutions. Energy-dispersive X-ray (EDX) detection of electrochemically treated $LiMn_2O_4$ proved the presence of the intercalated K^+ ion. The intercalation of the K^+ ion was partial, as is shown by the weight percent analysis of EDX detection results.

Introduction

The electrochemistry of $LiMn_2O_4$ in nonaqueous electrolytes has been extensively studied as a cathode material for rechargeable lithium batteries and, more specifically, for the rocking-chair type with carbon as the negative electrode. Lithium insertion characteristics of $LiMn_2O_4$ in nonaqueous electrolytes have been the subject of detailed investigations as a result of their importance in deciding the stability and reversibility in cycling.[1,2] Lithium can be inserted into or extracted from spinels by electrochemical or chemical redox reactions. The extraction of lithium from $LiMn_2O_4$ results in λ-MnO_2, while insertion produces $Li_2Mn_2O_4$.[3,4] This insertion induces the Jahn−Teller distortion of Mn^{3+} ions, favoring the phase transition from a cubic to a tetragonal structure. On the basis of NMR studies of lithium ion insertion into λ-MnO_2, Kanzaki et al. hypothesized that the Li exists in the atomic state but not in the ionic state. They also interpreted a reaction scheme of the insertion and extraction of lithium ions in λ-MnO_2 based on the potential−pH diagram; according to this scheme in aqueous solutions, lithium insertion occurs at a pH higher than 8.3 and lithium extraction occurs at a pH below 4.8.[5] A thorough investigation of lithium manganate materials by ^{6}Li and ^{7}Li magic-angle spinning NMR revealed that the Li^+ ion occupies both the tetrahedral and the octahedral sites of the spinel structure. Interestingly, it was shown that the materials synthesized at lower temperatures (550−650 °C) have defects in the normal spinel structure and do not undergo Jahn−Teller distortion, whereas the materials synthesized at higher temperatures (800 °C) undergo a cubic to tetragonal phase change below room temperature.[6] Employing the concept of the cooperative Jahn−Teller distortion, new materials such as $LiAl_xMn_{2-x}O_{4-\delta}F_z$ are prepared and investigated.[7]

The electrochemistry of $LiMn_2O_4$ in aqueous electrolytes has attracted the attention of only a few authors. The interest in the aqueous electrochemistry of $LiMn_2O_4$ arises as a result of the search for alternative Li-ion cells. The development of such cells starts with the studies related to the insertion behavior of protons and lithium ions into the $LiMn_2O_4$ structure and the subsequent structural changes associated with the redox process. Proton insertion in $LiMn_2O_4$ when cycled in KOH media is reported. Cyclic voltammetric and charge−discharge properties of undoped and Bi-doped $LiMn_2O_4$ in the 9 M KOH electrolyte revealed that Bi-doped spinels exhibit improved rechargeability.[8] In another work, lithium intercalation from the LiOH solution to form $Li_2Mn_2O_4$ from the host material of $LiMn_2O_4$ is described.[9] In a recent work by Cachet Vivier et al., they reported the reversible proton insertion in $LiMn_2O_4$ from borate buffer solutions. In contrast to Li insertion, proton insertion in the cubic lattice does not induce a cubic to tetragonal distortion.[10] In our earlier works, we reported the proton insertion behavior of $LiNiO_2$, $LiCoO_2$, and $LiMn_2O_4$ in alkaline solutions.[11,12]

It is known that the mode of synthesis plays a significant role in deciding the composition, structure, and physical and electrochemical properties of lithium manganate cathode materials. The importance of the synthesis conditions on the electrochemical performance of $LiMn_2O_4$ is well exploited by Tarascon et al. They synthesized the

* Author to whom correspondence should be addressed.
† Indian Institute of Chemical Technology.
‡ Ernst-Moritz-Arndt-Universität Greifswald.

(1) Thackeray, M.; Johnson, P.; de Picciotto, L.; Bruce, P.; Goodenough. J. B. *Mater. Res. Bull.* **1984**, *19*, 179.
(2) Thackeray, M.; de Picciotto, L.; de Kock, A.; Johnson, P.; Nicholas, V.; Dendorff, K. *J. Power Sources* **1987**, *21*, 1.
(3) David, W. I. F.; Thackeray, M. M.; de Picciotto, L.; Goodenough, J. B. *J. Solid State Chem.* **1987**, *67*, 316.
(4) Thackeray, M. M.; David, W. I. F.; Bruce, P. G.; Goodenough, J. B. *Mater. Res. Bull.* **1983**, *18*, 461.
(5) Kanzaki, Y.; Taniguchi, A.; Abe, M. *J. Electrochem. Soc.* **1991**, *138*, 333.
(6) Lee, Y. J.; Wang, F.; Grey, C. P. *J. Am. Chem. Soc.* **1991**, *120*, 12601.
(7) Amatucci, G. G.; Pereira, N.; Zheng, T.; Plitz, I.; Tarascon, J. M. *J. Power Sources* **1998**, *81−82*, 39.
(8) Schlörb, H.; Bungs, M.; Plieth, W. *Electrochim. Acta* **1997**, *42*, 2619.
(9) Li, W.; Mckinnon, W. R.; Dahn, J. R. *J. Electrochem. Soc.* **1994**, *141*, 2310.
(10) Cachet Vivier, C.; Bach, S.; Pereira Ramos, J. P. *Electrochim. Acta* **1999**, *44*, 2705.
(11) Mohan Rao, M.; Jayalakshmi, M.; Schäf, O.; Wulff, H.; Guth, U.; Scholz, F. *J. Solid State Electrochem.* **1999**, *4*, 17.
(12) Mohan Rao, M.; Jayalakshmi, M.; Schäf, O.; Wulff, H.; Guth, U.; Scholz, F. *J. Solid State Electrochem.* **2001**, *5*, 50.

10.1021/la0340448 CCC: $25.00
Published on Web 08/20/2003

materials by mechanochemical, low-temperature synthesis in ethylene glycol and a well-defined thermal treatment in air at 800 °C.[13−15] In a ethylene glycol medium, they showed that the nature of the cation inserted depends on the cationic content of the organic medium so that a variety of reduced MnO_2 compositions such as H_xMnO_2, (Li,H)-MnO_2, (Na,H)MnO_2, and (K,H)MnO_2 can be obtained.[14] In our earlier works,[11,12] we reported the preparation of $LiNiO_2$, $LiCoO_2$, and $LiMn_2O_4$ by a simple solution combustion technique. This technique has been used successfully for the preparation of ceramic and phosphor materials.[16,17]

In the present work, $LiMn_2O_4$ was synthesized by a low-temperature solution combustion technique and its composition was analyzed by X-ray diffraction (XRD) and inductively coupled plasma spectroscopy (ICP). To understand the intercalation electrochemistry of $LiMn_2O_4$ in neutral solutions, the solid was subjected to cyclic voltammetric and chronopotentiometric studies. Studies on the insertion electrochemistry of cations is essential because it is a preliminary step to understand the extent of the electrochemical reversibility of a redox reaction and to screen the material for its feasibility as an active battery electrode. To prove the metal cation intercalation, energy-dispersive X-ray (EDX) analysis of electrochemically treated samples of $LiMn_2O_4$ was carried out.

Experimental Section

Preparation of $LiMn_2O_4$ by the Low-Temperature Solution Combustion Technique. In this method, attention should be given to calculating the stoichiometric composition of oxidizing and reducing species to obtain phase-pure final products and also to avoid the evolution of undesired gases such as NO_2 during the combustion process. The stoichiometric compositions of the redox mixtures for the combustion reaction are calculated using the total oxidizing (O) and reducing (R) valencies of the individual components, which serve as the numerical coefficients for the stoichiometric balance, so that the equivalent ratio, R_e, is unity (i.e., O/R = 1) and the energy released by combustion is a maximum. On the basis of the concept used in propellant chemistry, the elements H, C, and M (Li, Mn) are considered reducing species with valencies +1, +4, +1 (Li), and +2 (Mn), respectively. The oxygen is considered an oxidizing species with a valency of −2, and the valency of nitrogen is considered 0. Accordingly, the oxidizing valencies of the $LiNO_3$ and $Mn(NO_3)_2$ compounds become −5 and −10, respectively, and the reducing valency of urea ($NH_2-CO-NH_2$) is +6. To get the value of R_e = 1, the moles of urea to be taken is calculated as

$$\text{oxidizing valencies of } LiNO_3 + 2Mn(NO_3)_2/\text{reducing valency of urea}$$

That is, (5 + 20)/6 = 4.166.

The stoichiometric equation for the synthesis of $LiMn_2O_4$ can be written as

$$LiNO_3 + 2Mn(NO_3)_2 + 4.2NH_2-CO-NH_2 \rightarrow LiMn_2O_4 + 13.4N_2 + 4.2CO_2 + 8.4H_2 + 3.4O_2$$

In a typical experiment, $Mn(NO_3)_2{\cdot}4H_2O$ (8.367 g), $LiNO_3$ (2.298 g), and urea (8.4 g) were dissolved in 50 mL of distilled water in a 500-mL glass beaker. The beaker was placed in a resistance-heated muffle furnace maintained at 500 °C. After a few minutes, the solution boiled and underwent rapid dehydration followed by decomposition with an intense flame to yield a fine black powder of $LiMn_2O_4$ (5.8 g). All the chemicals used were of analytical grade, and the solutions were prepared with double-distilled water.

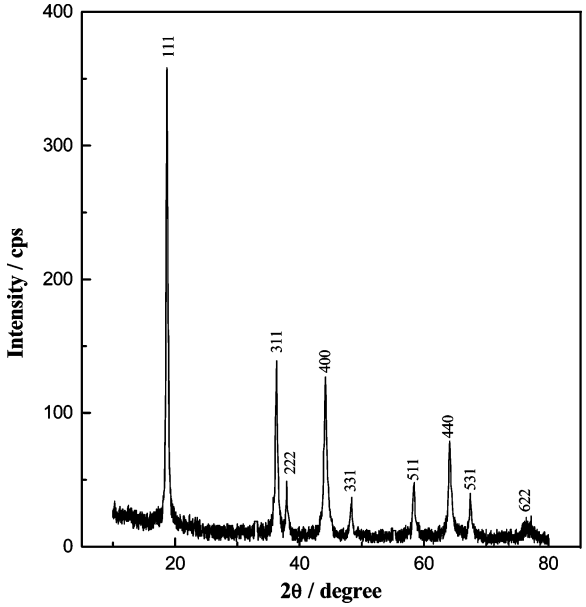

Figure 1. X-ray powder diffraction pattern of $LiMn_2O_4$ prepared by the solution combustion method.

Equipment and Measurements. For electrochemical measurements, the following instrumentation was used: an Autolab (ECO-Chemie, Utrecht, The Netherlands), an electrode stand VA 663 (Metrohm, Herisau, Switzerland), and a personal computer. The reference electrode (Metrohm, Switzerland) was an Ag/AgCl electrode with 3 M KCl (E = 0.208 V vs standard hydrogen electrode). Platinum wire was used as counter electrode. The solid $LiMn_2O_4$ powder was mechanically immobilized on the surface of the paraffin-impregnated graphite electrode (PIGE) and used as the working electrode. All the measurements were performed in solutions which were thoroughly deareated with high-purity nitrogen for at least 10 min. The voltammograms were recorded at 22 ± 1 °C. XRD measurements were performed with a HZG 4 (Seifert-SPM, Germany), and the scanning electron microscope (Leo 440, Germany) equipped with an Econ 4 detector (EDAX, U.S.A.) was used for the chemical analysis of the electrochemically treated samples of $LiMn_2O_4$.

Results and Discussion

XRD Studies. The XRD pattern of the $LiMn_2O_4$ sample prepared by the solution combustion technique is comparable with the standard Joint Committee on Powder Diffraction Standards data and shows the formation of a single-phase compound (Figure 1). It is reported in the literature that $LiMn_2O_4$ belongs to the spinel system with cubic symmetry ($Fd3m$). The chemical composition obtained by ICP analysis was $Li_{0.92}Mn_2O_4$. The deviation from the stoichiometry is due to the generation of a high temperature during the combustion, where volatile lithium loss can be expected. Our attempt to prepare stoichiometric $LiMn_2O_4$ by varying the lithium as well as urea concentrations by this method was not successful. The effect of the temperature on the synthesis of various Li−Mn-based oxide materials was reported by Lee et al.[6]

Electrochemical Studies. Before entering into the discussion part of explaining the origin of the two redox couples that appeared for $LiMn_2O_4$ in neutral electrolyte solutions, the stability of this compound in this pH and potential range has to be established. This exercise was necessary because the aqueous electrochemistry of this

(13) Tarascon, J. M.; Coowar, F.; Amatucci, G. G.; Shokoohi, F. K.; Guyomard, D. G. *J. Power Sources* **1995**, *54*, 103.
(14) Larcher, D.; Gerand, B.; Tarascon, J. M. *Int. J. Inorg. Mater.* **2000**, *2*, 389.
(15) Soiron, S.; Rougier, A.; Aymard, L.; Tarascon, J. M. *J. Power Sources* **2001**, *97−98*, 402.
(16) Kottaisamy, M.; Jayakumar, D.; Jagannathan, R.; Mohan Rao, M. *Mater. Res. Bull.* **1996**, *31*, 1013.
(17) Kottaisamy, M.; Mohan Rao, M.; Jayakumar, D. *J. Mater. Chem.* **1997**, *7*, 345.

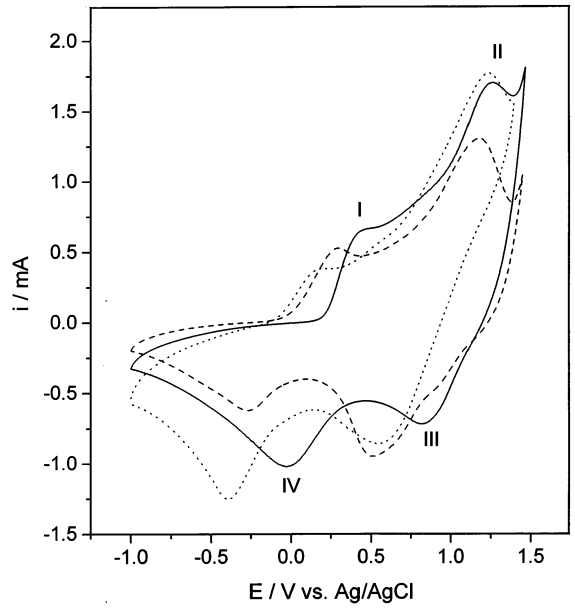

Figure 2. Cyclic voltammograms of mechanically immobilized $LiMn_2O_4$ on the surface of the PIGE in different 0.1 M neutral electrolyte solutions: scan rate = 0.05 V s^{-1}; (solid line) KCl; (dotted line) NH_4Cl; and (dashed line) LiCl.

compound was almost negligible, and the possibility of $LiMn_2O_4$ undergoing dissolution to produce the redox peaks in cyclic voltammograms cannot be excluded. From the potential−pH diagram of the $LiMn_2O_4$ system, the hypothetical standard electrode potential of $Li^+/LiMn_2O_4$ is 0.73 V versus the normal hydrogen electrode.[18] However, the experimental work done in the nonaqueous system does not validate this value. It was reported to be +4.2 V versus the Li^+/Li (metal) reference system, which was higher than the theoretical value of 3.73 V. This lack of coincidence is understandable because the preparation procedure concurrently affects the structure, morphology, and composition of the compound. The same fact influences the electrochemistry of $LiMn_2O_4$ in an aqueous medium. In an earlier work, MnO_2 was subjected to cathodic polarization in 5 M NH_4Cl solutions. A single peak at 1.35 V versus $Zn/ZnCl_2$ was reported, corresponding to the dissolution of MnO_2 particles.[19] Recently, electrochemical behavior of the thin-film $LiMn_2O_4$ electrode in aqueous media has been investigated, and the results indicate that the electrode was highly stable in aqueous media.[20] On the basis of the above evidences and inferences, we conclude that $LiMn_2O_4$ was stable within the potential limits and pH range of our experiment.

A few micrograms of solid $LiMn_2O_4$ powder synthesized by the solution combustion method was mechanically immobilized on the surface of the PIGE.[21] This technique is highly useful in determining the electrochemical characteristics of any new solid material because it need not be subjected to mechanical, physical, and chemical pretreatments. Cyclic voltammetric experiments in various concentrations of LiCl, KCl, and NH_4Cl electrolyte solutions and between the potential limits of −1 to +1.5 V versus Ag/AgCl were recorded. The scan rate employed was 0.05 V s^{-1}. Figure 2 shows the typical cyclic voltammograms obtained for the $LiMn_2O_4$ in 0.1 M KCl, LiCl, and NH_4Cl solutions. The cyclic voltammograms show two sets of redox peaks in all the electrolyte solutions. The formal potentials evaluated from the redox couples I−IV and II−III are presented in Table 1. The Li^+ ion, being the most electronegative cation, gets intercalated at more negative potentials compared to the K^+ and NH_4^+ ions. Hence, the increasing order of preference for cation intercalation in the $LiMn_2O_4$ lattice during electrochemical cycling was $Li^+ \gg K^+ > NH_4^+$. The observed difference in the formal potentials is due to different degrees of hydration of these cations. With an increase in concentration of the electrolyte solutions, the formal potentials for the redox couple I−IV increases in all three cases. However, for the K^+ and NH_4^+ ions against the Li^+ ion, the formal potentials of the second redox couple decreases with an increase in the concentration of the respective electrolyte solution. This could be due to the competitive proton insertion/extraction process that takes place with more ease in the presence of the K^+ and NH_4^+ ions. The shift of the electrode potentials toward the positive direction indeed indicates an increase in the free energy for the redox reaction.

Table 1. Formal Potentials of the $Mn^{3+/4+}$ System of Solid $LiMn_2O_4$ at Various Concentrations of KCl, LiCl, and NH_4Cl Electrolyte Solutions

	KCl		LiCl		NH_4Cl	
mol dm^{-3}	E_f(I−IV) (mV)	E_f(II−III) (mV)	E_f(I−IV) (mV)	E_f(II−III) (mV)	E_f(I−IV) (mV)	E_f(II−III) (mV)
0.05	9.5	1012	−43	800	153	1043
0.1	43.5	996	5.9	840	198	1041
0.3	99.5	985	81.2	890	260	1013
0.6	133	983	114	910	295	1005
1.0	149	983	153	920	321	1001

We believe that the redox peaks I and IV in the cyclic voltammograms in Figure 2 were due to the intercalation and deintercalation of the respective cations. Considering a typical example of the intercalation of the potassium ion, the equation for the redox reaction represented by peaks I and IV may be written as

$$xK^+ + LiMn_2O_4 + xe^- \rightarrow Li_{1-x}K_xMn_2O_4$$

In accordance with the Nernst law, this reaction should follow the dependence of the formal potential on the activity of the potassium cation:

$$E_f = E^0 + 0.059 \log a_{K^+}$$

That is, the formal potential $E_f = (E_a + E_c)/2$ (E_a, anodic peak potential; E_c, cathodic peak potential) of the redox reaction should be directly proportional to the concentration of K^+ ions in the KCl electrolyte solutions. This is found to be the case in all three electrolytes. Figure 3 shows the derived plots of E_f versus log [M^+] (M = K, Li, NH_4), where the straight line graph has a positive slope. The formal potentials taken to derive this plot were of the redox couple I−IV. So, in solid $LiMn_2O_4$, reversible intercalation of Li^+, K^+, and NH_4^+ ions takes place from neutral electrolyte solutions.

In nonaqueous electrolytes, $LiMn_2O_4$ was proved to undergo lithium insertion and reinsertion via two processes that were independent of each other.[22] In the present study dealing with the electrochemical behavior of $LiMn_2O_4$ in aqueous neutral electrolytes, cation intercalation takes place in two steps, as was realized by the two sets of redox couples shown in Figure 2. To understand

(18) Pourbaix, M. *Atlas of electrochemical equilibria in aqueous solutions*; Pergamon Press: New York, 1966.
(19) Ruetschi, P. *J. Electrochem. Soc.* **1976**, *123*, 495.
(20) Eftekhari, A. *Electrochim. Acta* **2001**, *47*, 495.
(21) *Electroanalytical chemistry, a series of advances*; Bard, A. J., Rubinstein, I., Eds.; Dekker: New York, 1998; Vol. 20, pp 1−86.
(22) Fiedler, D. A.; Besenhard, J. O.; Fooken, M. H. *J. Power Sources* **1997**, *69*, 11.

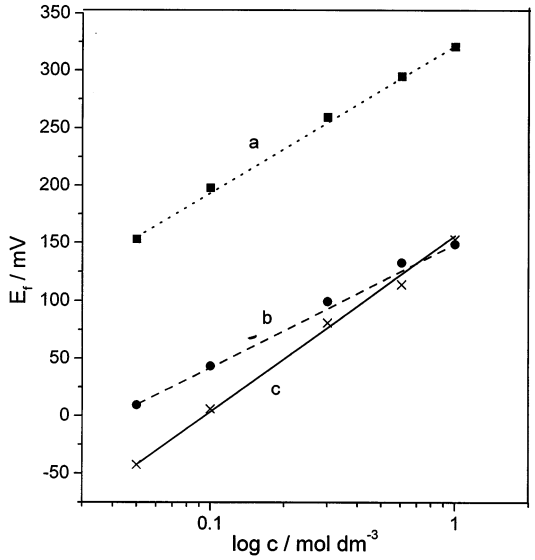

Figure 3. Derived plots of E_f versus log [M^+] in different electrolyte solutions: (a) NH_4Cl, (b) KCl, and (c) LiCl.

the electrochemistry of this system, it was necessary to verify whether the redox processes taking place were interdependent or independent of each other. If the redox processes, whatever they may be, occur independently, then the scanning of $LiMn_2O_4$ in their respective potential regions should produce redox peaks irrespective of one another. In the case of cation intercalation being a continuous process, the previously mentioned exercise would yield an electrochemical spectrum different from that in Figure 2. The results obtained out of this exercise were interesting and contrary to that in nonaqueous electrolytes. Cyclic voltammograms obtained in the two redox couple regions between the potential limits of −1.0 to +0.5 V and +0.5 to +1.3 V are shown in parts A and B of Figure 4, respectively. In Figure 4A, there was a single oxidation peak in the forward scan but no reduction peak in the reverse scan. In Figure 4B, there were no peaks either in the forward or in the backward scans. This result led us to the conclusion that peak II in the oxidation scan was formed as a result of subsequent oxidation of the resultant product at peak I. The oxidized product at peak II gets reduced at peak III, which again subsequently undergoes further reduction at peak IV. This continuity in the redox process gets perturbed when there is a discontinuity in the potential cycling, as is shown in Figure 4A,B.

In addition to the cyclic voltammetric experiments, $LiMn_2O_4$ was subjected to chronopotentiometric experiments in a 0.1 M KCl solution. This was done in view of providing supportive evidence to the two-step intercalation process observed in this work. Because the electrochemistry of $LiMn_2O_4$ in the aqueous medium was not well-studied, it becomes essential to confirm and augment the electrochemical results obtained through cyclic voltammetric experiments by some other electrochemical techniques. In chronopotentiometry, the variation of the potential of $LiMn_2O_4$ with time upon the application of a constant current was studied. A basic assumption is made that all the applied current initiates the reaction between $LiMn_2O_4$ and alkali metal cations in the solution, and the mass transfer is controlled by the diffusion of these cations. Although the change in the bulk concentration is negligible during the transient, the concentrations of both the

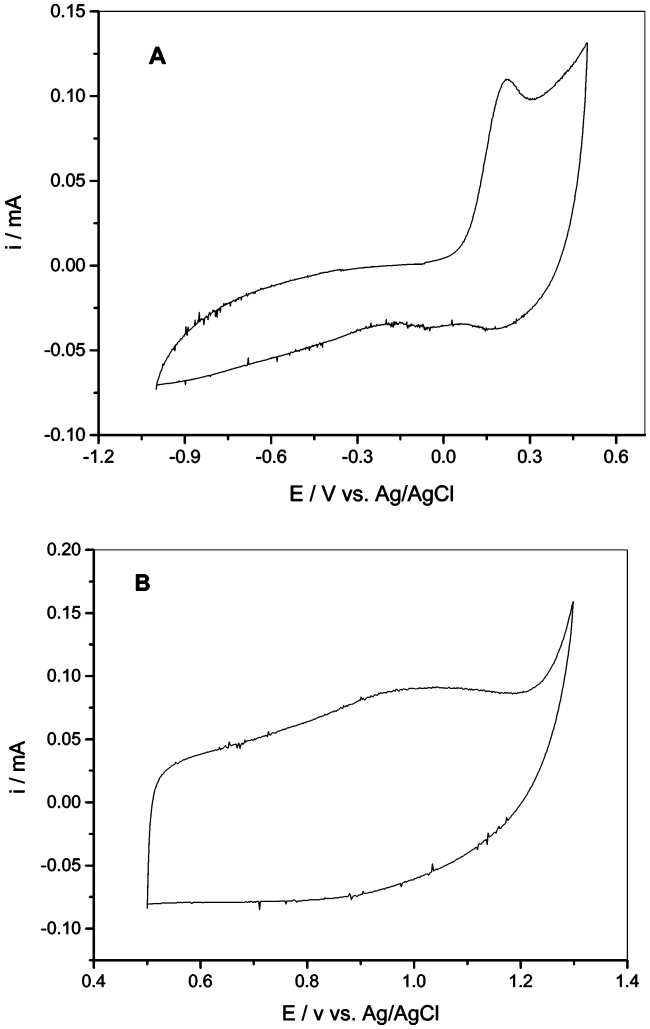

Figure 4. Cyclic voltammograms of mechanically immobilized $LiMn_2O_4$ on the surface of the PIGE in a 0.1 M KCl electrolyte solution at different potential ranges: scan rate = 0.05 V s^{-1}; (A) −1.0 to +0.5 V and (B) +0.5 to +1.3 V.

reactant and the product at the electrode surface vary markedly, and the ratio

$$C_{ox}(x = 0)/C_{red}(x = 0)$$

determines the observed potential. Eventually, the concentration of [ox] at the electrode surface has been reduced to 0, and diffusion is insufficient to supply enough reactant to satisfy the imposed current. At this point (the transition time), a large part of the current again charges the double layer and the potential shifts rapidly to a value at which some other electrode reaction occurs. During the passage of constant current, plateaus parallel to the *x* axis appear at the corresponding potential of the redox reaction of interest as steps that could be related to peaks in a cyclic voltammogram. Upon current reversal, the redox reaction proceeds in the opposite direction and the nature of the reversibility of a system can be determined. For battery electrodes such as Fe in Ni−Fe alkaline cells, this transient technique was extensively employed to understand the discharge behavior of iron in the presence of additives and to calculate the percentage utilization of active material.[23,24] Recently, for solid-state cells employing

(23) Jayalakshmi, N.; Muralidharan, V. S. *J. Power Sources* **1990**, *32*, 277.

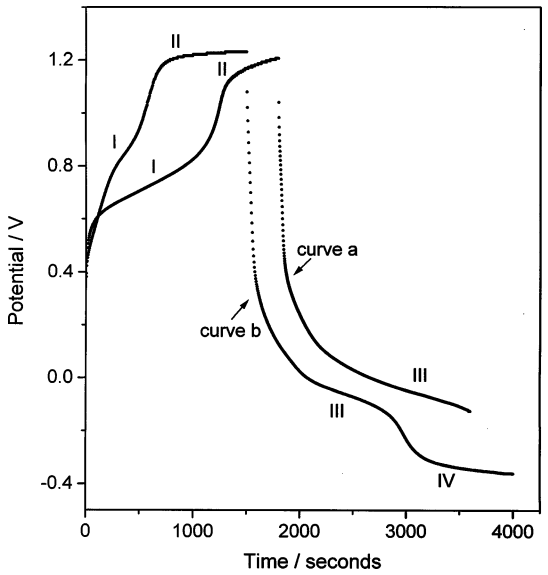

Figure 5. Double-step chronopotentiograms obtained for $LiMn_2O_4$ in a 0.1 M KCl solution.

Prussian blue and its analogues, double-step chronopotentiometry was employed to understand the changes in the reversible redox reactions over a long period of cycling.[25]

In the present work, double-step chronopotentiometry was carried out by passing a positive current of $+10\ \mu$A in the forward oxidation step and a negative current of $-10\ \mu$A in the backward reduction step. Initially, the time scale was set up to 1800 s under the assumption that both the oxidation and the reduction reactions would be completed within this time window. Curve a in Figure 5 shows the result of this experiment. In the forward oxidation step, there were two plateaus, I and II, in the potential ranges of 0.6−0.8 and 1.1−1.2 V, respectively. In the backward reduction step, there was a single plateau III in the potential range of 0 to −0.15 V. A fourth plateau did not appear as expected in this time scale. Henceforth in the subsequent experiment, the time scale was extended to 2000 s for each step. Curve b shows the chronopotentiogram obtained. In this time scale, there was a second plateau IV, suggesting that the oxidative steps in the forward scan were reversed during the reductive scan. There was a noticeable decrease in the transition times in the plateau I in curve b when compared to that of curve a, which may be understandable on the grounds that the reduction was not completed in curve a. As in cyclic voltammograms, if the reduction product at plateau IV gets oxidized at peak I in the oxidative step, then the decrease in the transition times in curve b can be understood. The transition time (τ), indeed, implies the percentage of applied current utilized for the faradic reaction of interest.

The previously mentioned results were interesting. Because the system is not a redox one in solution but an insertion material, it is difficult to assign the exact valence state for each species and to separate the effect of cations from that of electrons upon the redox potentials. Mostly, redox potentials are determined on the basis of the transfer of a cation across the solid/liquid interface, which in turn would reflect the identity of the cation and the ease with which the reaction occurs. So, it becomes all the more difficult to ascertain a particular reason to explain the abnormal behavior of cation intercalations. The formal potentials of the redox peaks of II and III in the cases of K^+ and NH_4^+ ions decrease with an increase of the concentration of the electrolyte solutions, as is evidenced from Table 1. This could be as per the Nernst law as a result of proton intercalation taking place in these peak regions, as was established in the cases of $LiNiO_2$, $LiCoO_2$,[11,12] and $LiMn_2O_4$.[10] Then the redox reactions responsible for the redox couples I−V and II−III may be represented by eqs 1 and 2 as

$$xK^+ + LiMn_2O_4 + xe^- \rightleftarrows Li_{1-x}K_xMn_2O_4 \qquad (1)$$

$$xH^+ + LiMn_2O_4 + xe^- \rightleftarrows Li_{1-x}H_xMn_2O_4 \qquad (2)$$

In accordance with the literature and experimental evidence, we put forward the previous scheme of redox equations for the two-step intercalation of the cations, each step corresponding to its occupation in two different sites of crystal structure. Having established this fact, the next step was to solve the puzzle of why the redox couples were interdependent of one another, as was evidenced in Figure 4. At the $LiMn_2O_4$/solution interface, when the oxidation step involving the formation of peak I occurs as a result of anodic polarization, K^+ ions, electrons, and water molecules coexist until further polarization proceeds. Upon the continuation of anodic polarization, potassium ions may get adsorbed at some site (S) of the lithium manganate electrode surface and react with water molecules to produce protons and hydroxyl ions as represented by the following equations:

$$K^+ + e^- \rightarrow K(S)$$

$$K(S) + H_2O \rightarrow K^+ + S + H^+ + OH^-$$

The resultant protons formed out of this reaction undergo the intercalation process to form peak II as

$$H^+ + LiMn_2O_4 + e^- \rightarrow LiHMn_2O_4$$

This phenomenon explains why the redox couples I−IV and II−III were interdependent on one another and why we did not observe any peaks in Figure 4B when the experiment was carried out in that particular potential range. Because of the above changes taking place at the interface, the pH at the interface varies substantially from that of the bulk pH, which provides a favorable condition for the intercalation of protons in lithium manganate.

Though this kind of mechanism appears to be new in intercalation electrochemistry, it is a well-known phenomenon in passivation and corrosion aspects of electrochemistry. To cite a few examples, it was observed that on solid iron, the rate of hydrogen evolution decreases with KOH concentration.[26] Also, the hydrogen evolution reaction on zinc, iron, and tin was found to occur with the discharge of alkali metal ions being the slow step in the alkali solutions.[27] On an iron oxide surface, hydrogen

(24) Jayalakshmi, N.; Muralidharan, V. S. *J. Power Sources* **1990**, *32*, 341.

(25) Jayalakshmi, M.; Scholz, F. *J. Power Sources* **2000**, *91*, 217.

(26) Kalaignan, G. P.; Muralidharan, V. S.; Vasu, K. I. *Proceedings of the Annual Technical Meeting, Electrochemical Society of India* **1985**, 32.

(27) Muralidharan, V. S.; Rajagopalan, K. S. *J. Electroanal. Chem.* **1978**, *24*, 21.

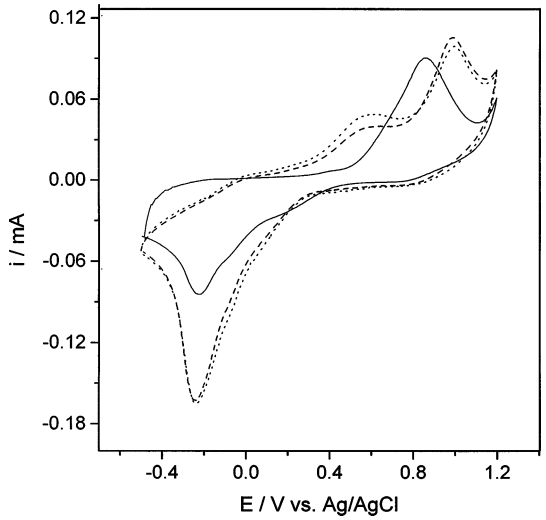

Figure 6. Cyclic voltammograms obtained for $LiMn_2O_4$ in a 0.1 M KCl solution: scan rate = 1 mV s^{-1}; (solid line) first cycle; (dashed line) second cycle; and (dotted line) third cycle.

evolution takes place with the discharge of K^+ ions as follows:[28]

$$K^+ + e^- \rightarrow K(S)$$

$$K(S) + H_2O \rightarrow K^+ + S + H_{ads} + OH^-$$

$$2H_{ads} \rightarrow H_2$$

where S is the oxide surface site. In neutral solutions employed in the present study, hydrogen undergoes the intercalation process instead of the evolution process.

Another interesting result that confirms the above hypothesis was the cyclic voltammograms obtained for $LiMn_2O_4$ in KCl solutions at a slow scan rate (Figure 6). Only one set of redox peaks appeared in all the scans. This was understandable because the time window provided to complete the intercalation process was long and whatever species formed at the interface would diffuse into the solution or get irreversibly trapped in the oxide lattice.

Last, to confirm our hypothesis of alkali metal cation intercalation in $LiMn_2O_4$, EDX studies of electrochemically treated electrodes were carried out. The PIGE electrode immobilized with $LiMn_2O_4$ was cycled in a 0.1 M KCl solution and then subjected to EDX detection. The results showed that the cycled $LiMn_2O_4$ electrode contains potassium ions in it. If the replacement of lithium by potassium ions was 100%, then the weight percents of K and Mn should be 26.2 and 73.8, respectively, whereas from the EDX results, we found that the weight percents of K and Mn were 4.05 and 95.95, respectively, indicating that the replacement of lithium by potassium ions was partial. This type of partial proton insertion was reported for spinel $LiMn_2O_4$, and the composition of the cathode material after the first charge (charge/discharge) studies was noted to be $H_{0.35}Li_{0.7}MnO_2$. Poor efficiency of the oxidation process was attributed to the irreversible trapping of protons in the oxide lattice.[10] This observation is consistent with our present work.

Conclusions

Lithium manganate was prepared by a simple low-temperature solution combustion method. This method is highly advantageous over the conventional ones because it is cost- and time-effective. The ICP analysis showed the material to have a composition of $Li_{0.92}Mn_2O_4$. Electrochemical studies revealed the dual cation insertion/extraction. Potassium ion insertion in $LiMn_2O_4$ from a neutral electrolyte solution is reported for the first time. Along with protons, K^+, Li^+ and NH_4^+ ions were intercalated into the lithium manganate structure. EDX results of electrochemically treated samples proved the presence of potassium ions in $LiMn_2O_4$. The ion exchange of lithium by potassium remains partial.

Acknowledgment. M.J. acknowledges provision of a fellowship from Humboldt Stiftung (AvH) and M.M.R. acknowledges a postdoc fellowship from Deutsche Forschungsgemeinschaft (DFG).

LA0340448

(28) Jayalakshmi, M.; Muralidharan, V. S. *Proceedings of the Indian Academy of Sciences* **1991**, *103* (2), 161.